INCREASING ACHIEVABLE INFORMATION RATES WITH PILOT-BASED DSP IN STANDARD INTRADYNE DETECTION

Yuta Wakayama[1,2], Eric Sillekens[1], Lídia Galdino[1], Domaniç Lavery[1], Robert I. Killey[1] and Polina Bayvel[1]*

[1]*Optical Networks Group, Department of Electronic and Electrical Engineering, University College London, Torrington Place, London WC1E 7JE, United Kingdom*
[2]*KDDI Corporation, 3-10-10 Iidabashi, Tokyo 102-8460, Japan*
**E-mail: yu-wakayama@kddi.com*

Keywords: DIGITAL SIGNAL HANDLING TECHNIQUES

Abstract

Information rates of up to 17.4 b/4D-symbol and 15.9 b/4D-symbol were achieved at 15 GBd and 30 GBd, with pilot overhead of less than 5%. Information rates exceed previous results with 8-bit DACs while symbol rates were doubled.

1 Introduction

Information rates in coherent optical communication systems can be increased by employing higher-order quadrature amplitude modulation (QAM) formats, provided that the transmission system has sufficient signal-to-noise ratio (SNR) to do so [1–3]. Often the received SNR is limited by the electrical and optical noise of the transceiver subsystems and the achievable information rates (AIRs) are, thus, bound by the back-to-back performance. The contribution of quantisation noise and other electrical noise sources limits the effective number of bits (ENOB) of digital-to-analogue converters (DACs) and analogue-to-digital converters (ADCs) [4–7]. In the optical domain, laser phase noise restricts the effective received SNR as it incurs errors in equalisation and carrier-phase recovery [8–11]. Pilot-based digital-signal processing (DSP) allows the implementation of high-order QAM in standard intradyne configurations [12, 13], in which digital pilot symbols are embedded within the data payload instead of using a separate optical pilot tone. This approach avoids the requirement for modifications to the optical configuration while making it possible to implement effective equalisation and carrier-phase recovery with a low computational complexity [14, 15]. Recently, AIR upper bound values of 15.9 b/4D-symbol for uniform 1024 QAM and 16.8 b/4D-symbol for probabilistically-shaped 1024 QAM have been reported for back-to-back configurations with 8-bit DACs, driven at 8 GBd [16].

In this paper, we present a pilot-based DSP chain for achieving a further significant increase in AIR. We experimentally demonstrate 15 GBd and 30 GBd dual-polarisation (DP) 64/256/1024 QAM transceivers in a standard coherent intradyne configuration with 8-bit DACs and ADCs. We show that by applying the proposed DSP chain to a geometrically-shaped (GS) DP-1024 QAM, the achievable information rate at 15 GBd can be increased by 1.9 b/4D-symbol, up to 17.4 b/4D-symbol.

2 Experimental Setup and Pilot-Based DSP

The experimental setup is shown in Fig. 1(a). Two external cavity lasers (ECLs) with a linewidth of <100 kHz and frequency of 193.4 THz were used as the transmitter source and local oscillator (LO). The signal was modulated by a DP-IQ modulator. The electrical signal was generated by DACs driven at 90 GSa/s for both 15 GBd and 30 GBd and supported by linear amplifiers. The modulated optical signal was followed by an Er-doped fiber amplifier and a variable optical attenuator (VOA) and combined with an amplified spontaneous emission (ASE) source. The optical signal-to-noise ratio (OSNR) can be swept up to 43 dB (noise bandwidth: 0.1 nm) by adjusting VOAs. The receiver was configured with a polarisation-diverse optical 90-degree hybrid, balanced detectors and oscilloscopes. At a 15 GHz carrier frequency, the measured ENOB of the DAC was 5 bits and the ENOB of the ADCs was 4.8 bits [6, 7].

In this work, we considered uniform 64/256/1024 QAM and GS-1024 QAM. The GS constellation was designed using a gradient descent algorithm to maximise generalised mutual information (GMI) at an SNR of 28 dB (see Fig. 4) [17]. GMI was chosen as the target metric as it provides an upper bound to information rate under the assumption of a binary soft-decision decoder [18]. Due to the size of the constellation, it was computationally infeasible to reassign the bit-to-symbol mapping with each optimisation step [19], so the optimisation algorithm was instead initialised with Gray-labelled uniform 1024 QAM, which is known to be a good mapping at high SNRs. (The optimised constellation is shown inset in Fig. 4.)

The signal was spectrally shaped with a root-raised cosine filter (roll-off: 0.01) and nonlinear pre-emphasis [20]. In addition, QPSK modulated pilot symbols were embedded to construct a data frame as shown in Fig. 1(b). The set of pilot symbols at the head of the data frame form a pilot sequence, which is used for frame synchronisation and equalisation [14]. On the other hand, pilot symbols inserted at pilot rate N_c^{-1} within the payload are used for carrier-phase estimation (CPE). Figure 1(c) displays the receiver side DSP chain. After resampling to 2 Sa/symbol and synchronisation, the equaliser is trained on the pilot sequence, using two algorithms. Both algorithms use only the pilot sequence (N_s samples) for data aided channel estimation. First, the recursive least squares (RLS) algorithm is applied for its extremely fast convergence time [21]. Then the pilot symbols are passed to the least mean squares (LMS) algorithm with progressively smaller learning parameters to reduce the final error of the inverse channel estimate. The trained filter taps are applied for the rest of the received samples, only tracking the channel with LMS updates using the CPE-pilot symbols. Then the signals are demultiplexed into the two polarisations. After frequency offset estimation/equalisation (FOE), a two-step CPE algorithm is implemented. In the first step, the phase noise of the pilot symbols is estimated and linearly interpolated between pilot symbols, where the last symbol of the pilot sequence is also employed as a pilot symbol for CPE. Assuming N_c is sufficiently small compared to the temporal evolution of phase noise, linear interpolation compensates for the majority of the phase noise. However, the residual phase noise reduces the potential SNR and induces instability for data estimation. To mitigate this, we implemented residual phase estimation (RPE) based on the maximum-likelihood (ML) algorithm as the second stage CPE [22]. Finally, after applying the Gram-Schmidt orthogonalisation procedure (GSOP), the AIR was estimated by deducting the pilot overhead (OH) from the GMI, where OH can be defined as $[N_s + (N_f - N_s)/N_c]/N_f$. Note that OH depends on the frame length N_f and, in our experiment, was limited by the memory size of the arbitrary waveform generators. In our setup, 85312 and 170624 were the maximum symbol sequence lengths at 15 GBd and 30 GBd, respectively. The frame length was fixed at $N_f = 65536$ for both symbol rates in the optimisation process.

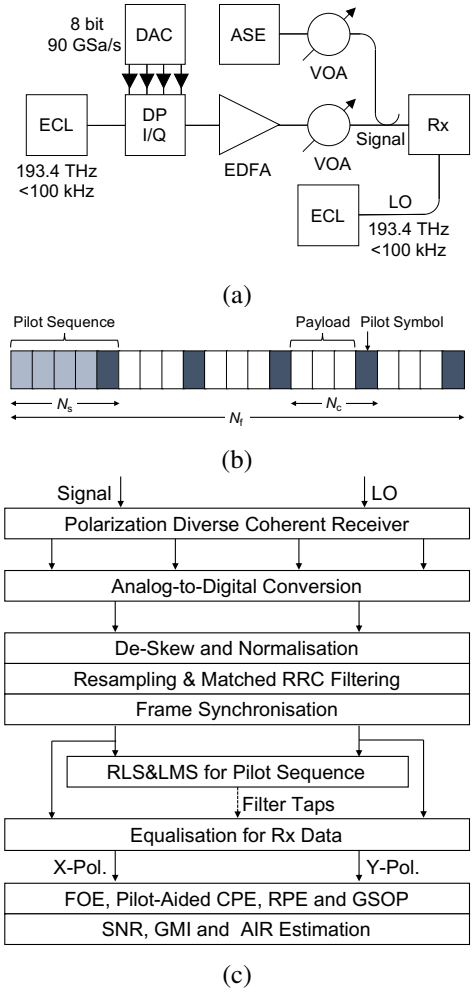

Fig. 1. Experimental setup and pilot-based DSP chain.

3 Required Pilot Overhead and AIR

The required total OH is expected to be dependent on the modulation format, symbol rate, received SNR, linewidth and nonlinear impairments [22–24]. The parameters N_s and N_c can be individually optimised to maximise AIR [14]. First, the pilot sequence length N_s was swept at the maximum SNR while the

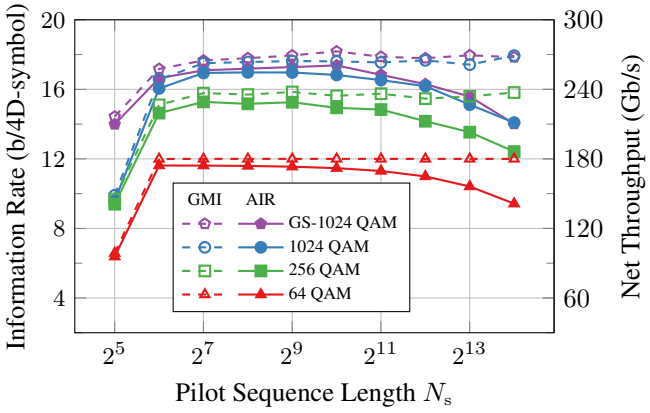

Fig. 2. Information Rate vs Pilot Sequence Length at 15 GBd.

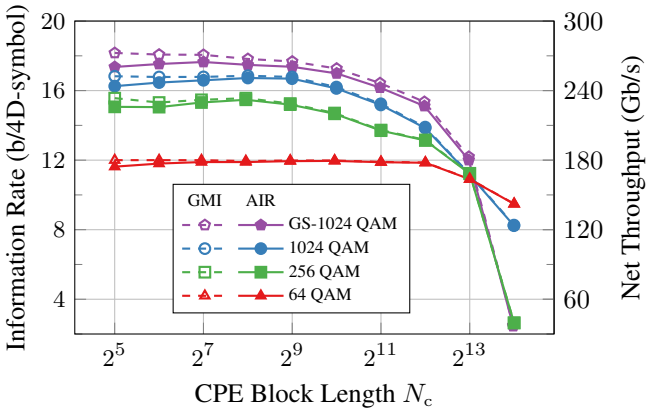

Fig. 3. Information Rate vs CPE Block Length at 15 GBd.

Table 1 AIR gain for 1024 QAM at 15 GBd.

Change	AIR gain (b/4D-symbol)
RLS	+0.4
LMS	+0.7
RPE	+0.1
GS	+0.7
Total	+1.9

CPE block length and the frame length were fixed at $N_c = 32$ and $N_f = 65536$ (Fig. 2). All curves show similar trends. For each modulation format, GMI was almost saturated, even when N_s was only 64 symbols. By increasing N_s, GMI would be completely saturated; however, AIRs were decreased due to the larger OH. Secondly, the pilot rate N_c was swept to further increase AIR at specific pilot sequence lengths (Fig. 3). The AIRs were maximised at $N_s = 64, 128, 256, 1024$ for 64 QAM, 256 QAM, 1024 QAM and GS-1024 QAM, respectively. By increasing N_c, CPE accuracy was degraded and residual phase noise would reduce both the GMI and AIR. Due to the high SNR, the GMI of 64 QAM was still saturated (>11.9 b/4D-symbol) even if $N_c = 2046$ (total OH: 0.15%). The maximum AIRs for 256 QAM and 1024 QAM were 15.5 b/4D-symbol (total OH: 0.59%) and 16.7 b/4D-symbol (total OH: 0.78%) at $N_c = 256$. As for GS-1024 QAM, the maximum AIR of 17.5 b/4D-symbol was observed at $N_c = 128$ (total OH: 2.3%). The similar AIR was observed when $N_c < 128$. The realised gain in AIR for 15-GBd DP-1024 QAM at $N_s = 256$ and $N_c = 256$ (OH: 0.78%) is summarised in Table 1, compared to a pilot-based DSP with a constant modulus algorithm (CMA) for equalisation and linear interpolation only for CPE. The nonlinear pre-emphasis at the transmitter provided a large gain of 1.6 b/4D-symbol. At the receiver side, by introducing LMS, the AIR was improved by 0.7 b/4D-symbol compared to a CMA based equalisation. In addition, RLS gained 0.4 b/4D-symbol. Furthermore, RPE can increase AIR by 0.1 b/4D-symbol compared to linear interpolation only. In total, AIR was increased by 3.5 b/4D-symbol.

Figure 4 and 5 show measured AIR for a range of SNRs at 15 GBd and 30 GBd, respectively. The pilot parameters were fixed at $N_s = 1024$ and $N_c = 32$. The observed maximum SNRs of 1024 QAM at 15 GBd and 30 GBd were bound at 29 dB and 26 dB, respectively. Although the QAM orders are greatly different between 64 QAM and 1024 QAM, the difference in the maximum SNRs was 0.5 dB for both symbol rates. For SNRs of >17 dB, the AIR of GS-1024 QAM became higher than that of the other formats at both symbol rates. The linear regime for each curve is along the line of $2\log_2(1 + \mathrm{SNR})$, as expected [2] and indicates that the implementation penalty of our DSP chain was low.

Finally, we confirmed that the AIRs of GS-1024 QAM with the maximum frame lengths at 15 GBd and 30 GBd reached 17.4 b/4D-symbol and 15.9 b/4D-symbol, where $N_s = 1024$, $N_c = 32$ for both symbol rates and pilot OH were 4.3% and 3.7%, respectively. As a result, we observed net throughputs of 261 Gb/s and 477 Gb/s at 15 GBd and 30 GBd, respectively.

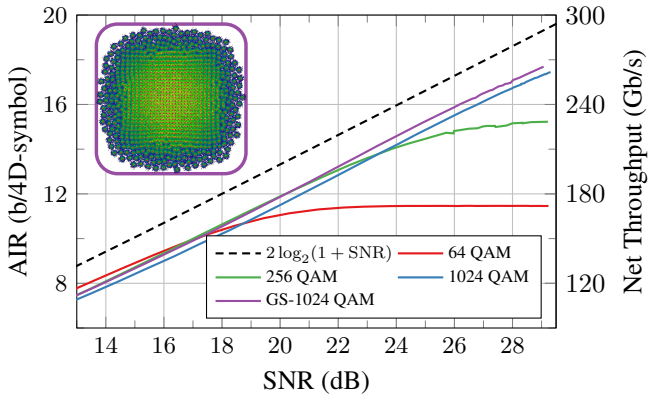

Fig. 4 Experimentally measured AIR vs SNR at 15 GBd ($N_s = 1024$, $N_c = 32$).

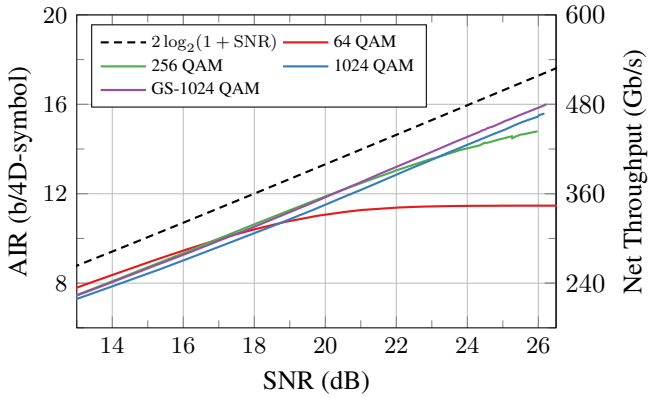

Fig. 5 Experimentally measured AIR vs SNR at 30 GBd ($N_s = 1024$, $N_c = 32$).

4 Conclusion

We have proposed a pilot-based digital signal processing chain and investigated its performance for dual-polarisation (DP) 64/256/1024 quadrature amplitude modulation (QAM) and geometically-shaped (GS) DP-1024 QAM at 15 GBd and 30 GBd in a back-to-back conventional intradyne configuration. We observed high signal-to-noise ratios of 29 dB and 26 dB for 1024 QAM at 15 GBd and 30 GBd, respectively. The total gain in the achievable information rate (AIR) was +3.5 b/4D-symbol and has been experimentally demonstrated by combining nonlinear preemphasis, RLS, LMS, RPE and a GS constellation. Moreover, the required pilot overhead of less than 5% has been experimentally achieved for each QAM format. We have determined new upper bounds on AIRs of 17.4 b/4D-symbol and 15.9 b/4D-symbol at 15 GBd and 30 GBd, respectively, which correspond to AIR exceeded previous work [16] with 8-bit digital-to-analogue converters while symbol rates were doubled or more. These result in the throughput values of 261 Gb/s and 477 Gb/s for a single carrier transmission at 15 GBd and 30 GBd, respectively.

Support for this work is from UK EPSRC TRANSNET Programme Grant (EP/R035342/1) and by RAEng Research Fellowships (D. Lavery, L. Galdino).

References

[1] C. Laperle and M. OSullivan, "Advances in high-speed DACs, ADCs, and DSP for optical coherent transceivers," *Journal of Lightwave Technology*, vol. 32, no. 4, pp. 629–643, Feb. 2014.

[2] R. Maher, A. Alvarado, D. Lavery, and P. Bayvel, "Increasing the information rates of optical communications via coded modulation: a study of transceiver performance," *Scientific Reports*, vol. 6, no. 1, Feb. 2016.

[3] R. Maher, M. Torbatian, S. Koenig *et al.*, "Constellation shaping for high symbol rate SNR limited transceivers," in *Next-Generation Optical Communication: Components, Sub-Systems, and Systems VIII*, G. Li and X. Zhou, Eds. SPIE, Feb. 2019.

[4] X. Chen, S. Chandrasekhar, S. Randel *et al.*, "Experimental quantification of implementation penalties from limited adc resolution for Nyquist shaped higher-order QAM," in *2016 Optical Fiber Communications Conference and Exhibition (OFC)*, March 2016, p. W4A.3.

[5] S. Varughese, J. Langston, V. A. Thomas *et al.*, "Frequency dependent ENoB requirements for m-QAM optical links: An analysis using an improved digital to analog converter model," *Journal of Lightwave Technology*, vol. 36, no. 18, pp. 4082–4089, Sep. 2018.

[6] L. Galdino, D. Lavery, Z. Liu *et al.*, "The trade-off between transceiver capacity and symbol rate," in *2018 Optical Fiber Communications Conference and Exposition (OFC)*, March 2018, p. W1B.4.

[7] L. Galdino, D. Semrau, D. Lavery *et al.*, "On the limits of digital back-propagation in the presence of transceiver noise," *Optics Express*, vol. 25, no. 4, p. 4564, Feb. 2017.

[8] Y. Koizumi, K. Toyoda, M. Yoshida, and M. Nakazawa, "1024 QAM (60 gbit/s) single-carrier coherent optical transmission over 150 km," *Optics Express*, vol. 20, no. 11, p. 12508, May 2012.

[9] S. Beppu, K. Kasai, M. Yoshida, and M. Nakazawa, "2048 QAM (66 Gbit/s) single-carrier coherent optical transmission over 150 km with a potential SE of 153 bit/s/Hz," *Optics Express*, vol. 23, no. 4, p. 4960, Feb. 2015.

[10] S. Okamoto, M. Terayama, M. Yoshida *et al.*, "Experimental and numerical comparison of probabilistically shaped 4096 QAM and a uniformly shaped 1024 QAM in all-raman amplified 160 km transmission," *Optics Express*, vol. 26, no. 3, p. 3535, Feb. 2018.

[11] M. Mazur, J. Schroder, A. Lorences-Riesgo *et al.*, "12 b/s/Hz spectral efficiency over the C-band based on comb-based superchannels," *IEEE Journal of Lightwave Technology*, vol. 37, no. 2, pp. 411–417, Jan. 2019.

[12] R. Maher, K. Croussore, M. Lauermann *et al.*, "Constellation shaped 66 GBd DP-1024QAM transceiver with 400 km transmission over standard SMF," in *2017 European Conference on Optical Communication (ECOC)*, Sep. 2017, paper Th.PDP.B.2.

[13] S. L. Olsson, J. Cho, S. Chandrasekhar *et al.*, "Probabilistically shaped PDM 4096-QAM transmission over up to 200 km of fiber using standard intradyne detection," *Optics Express*, vol. 26, no. 4, p. 4522, Feb. 2018.

[14] M. Mazur, J. Schroder, A. Lorences-Riesgo *et al.*, "Optimization of low-complexity pilot-based DSP for high spectral efficiency 51×24 Gbaud PM-64QAM transmission," in *2018 European Conference on Optical Communication (ECOC)*, Sep. 2018, p. Mo4F.2.

[15] E. Börjeson, C. Fougstedt, and P. Larsson-Edefors, "ASIC design exploration of phase recovery algorithms for m-QAM fiber-optic systems," in *Optical Fiber Communication Conference (OFC) 2019*. OSA, 2019, p. W3H.7.

[16] E. P. da Silva, F. Klejs, M. Lillieholm *et al.*, "Experimental characterization of 10×8 GBd DP-1024QAM transmission with 8-bit DACs and intradyne detection," in *2018 European Conference on Optical Communication (ECOC)*, Sep. 2018, p. Th1D.3.

[17] M. Ionescu, D. Lavery, A. Edwards *et al.*, "74.38 Tb/s transmission over 6300 km single mode fiber with hybrid EDFA/raman amplifiers," in *Optical Fiber Communication Conference (OFC) 2019*. OSA, 2019, p. Tu3F.3.

[18] A. Alvarado, E. Agrell, D. Lavery *et al.*, "Replacing the soft-decision FEC limit paradigm in the design of optical communication systems," *Journal of Lightwave Technology*, vol. 33, no. 20, pp. 4338–4352, Oct. 2015.

[19] B. Chen, Y. Lei, D. Lavery *et al.*, "Rate-adaptive coded modulation with geometrically-shaped constellations," in *2018 Asia Communications and Photonics Conference*, October 2018, p. S3K.5.

[20] P. W. Berenguer, M. NÃűlle, L. Molle *et al.*, "Nonlinear digital pre-distortion of transmitter components," *Journal of Lightwave Technology*, vol. 34, no. 8, pp. 1739–1745, April 2016.

[21] S. Haykin, *Adaptive Filter Theory (4th Ed.)*. Prentice-Hall, Inc., 2002.

[22] A. Spalvieri and L. Barletta, "Pilot-aided carrier recovery in the presence of phase noise," *IEEE Transactions on Communications*, vol. 59, no. 7, pp. 1966–1974, July 2011.

[23] M. Magarini, L. Barletta, A. Spalvieri *et al.*, vol. 24, no. 9, pp. 739–741, May 2012.

[24] M. P. Yankov, L. Barletta, and D. Zibar, "Phase noise compensation for nonlinearity-tolerant digital subcarrier systems with high-order QAM," *IEEE Photonics Journal*, vol. 9, no. 5, pp. 1–12, Oct. 2017.